

# Organic & Biomolecular Chemistry

Accepted Manuscript



This is an *Accepted Manuscript*, which has been through the Royal Society of Chemistry peer review process and has been accepted for publication.

*Accepted Manuscripts* are published online shortly after acceptance, before technical editing, formatting and proof reading. Using this free service, authors can make their results available to the community, in citable form, before we publish the edited article. We will replace this *Accepted Manuscript* with the edited and formatted *Advance Article* as soon as it is available.

You can find more information about *Accepted Manuscripts* in the [Information for Authors](#).

Please note that technical editing may introduce minor changes to the text and/or graphics, which may alter content. The journal's standard [Terms & Conditions](#) and the [Ethical guidelines](#) still apply. In no event shall the Royal Society of Chemistry be held responsible for any errors or omissions in this *Accepted Manuscript* or any consequences arising from the use of any information it contains.

## ARTICLE

## 3D shapes of aryl(dihydro)naphthothiophenes: a comprehensive and structural study

Cite this: DOI: 10.1039/x0xx00000x

H. Boufroura,<sup>a</sup> A. Souibgui,<sup>a,c</sup> A. Gaucher,<sup>a</sup> J. Marrot,<sup>a</sup> G. Pieters,<sup>b</sup> F. Aloui,<sup>c</sup> B. Ben Hassine,<sup>c</sup> G. Clavier,<sup>d</sup> and D. Prim<sup>a</sup>

Received 00th January 2012,  
Accepted 00th January 2012

DOI: 10.1039/x0xx00000x

www.rsc.org/

A convenient access to new aryl(dihydro)naphthothiophenes is described using a common  $\beta$ -chloroacroleine derivative. Our strategy is based on the construction of a condensed thiophene ring prior to a Suzuki-Miyaura coupling and allowed installing various substituents at the molecular platform. The overall shapes of these architectures were confirmed by X-ray analyses and were in good agreement with theoretical calculations. It has been established that the relative orientation between all fragments that composed molecules within this series is strongly related to both steric and electronic factors. Contribution of these key parameters revealed crucial to rationalize attempts to prepare fluorenone and fluorene derivatives from aryl(dihydro)naphthothiophene platforms.

### Introduction

Naphthalene is a pivotal platform in the construction of elaborated molecular architectures. In this context, naphthalene cores substituted by one (or more) aryl groups are especially attractive. Naphthalene units appear rigid and strictly planar in the well-known aryl-naphthalene or binaphthyl series for example. Their 3D-templating-shape revealed beneficial in several domains relying on the use of binaphthyl-like scaffolds for example such as catalysis,<sup>1</sup> chiroptical switch and/or molecular recognition,<sup>2</sup> dendrimers and polymers.<sup>3</sup> In contrast, 1,8-diarylnaphthalenes display a distorted naphthalene scaffold. These representative examples exhibit a peculiar topology in which cofacial aromatic groups installed at the naphthalene core set the overall shape of the architecture (figure 1).

In this context, it has been recently shown that 1,8-diraylnaphthalenes may exist through several conformers for *ortho*, *ortho* disubstituted structures.<sup>4,5</sup> Further, the overall topology is depending on steric factors and electronic contributions and/or interactions between both aromatic groups<sup>4</sup> in good agreement with recent theoretical calculations.<sup>5</sup> Interestingly, X-ray analysis of several 1,8-diraylnaphthalenes showed that the naphthalene platform is able to deform itself and absorb one part of the steric congestion enforced by the presence of two aryl groups. Deformation of the naphthalene unit can be estimated by mean of key parameters such as dihedral angles as shown in figure 1. We contributed to this research area by the construction of elaborated molecular architectures including planar, twisted and helical shapes<sup>6</sup> and their applications.<sup>7</sup> The flexible vs rigid balance of substituted naphthalenes is undoubtedly a key feature that contributed to the renowned of such platforms. In deep contrast, less is known about the overall shape of naphthalene derivatives bearing one aryl group and incorporating a fused heterocycle. Though such architectures have been shown appealing precursors for the preparation of fused fluorenones<sup>8</sup> and the naphthothiophene core displaying performance-enhancing ability in artificial energy conversion devices.<sup>9</sup> In this context, we report herein the preparation of several naphtho- and dihydronaphthothiophene derivatives bearing aromatic substituents at the peri position of the molecular platform (figure 1-3). X-ray in the solid state as well as theoretical calculations have been realized in order to gain informations concerning the overall topology of the molecular platform such as (i) the shape of the (dihydro)naphthalene core (ii) the spatial

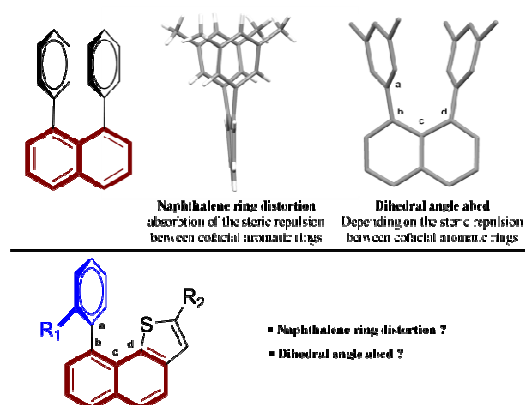


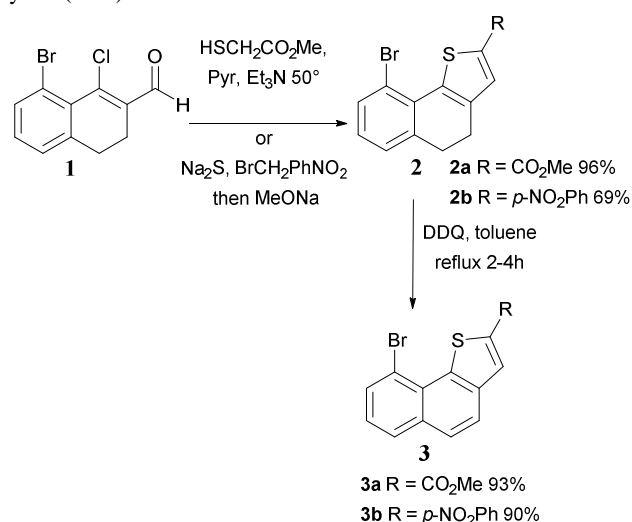
Figure 1. Deformation of naphthalene unit in 1,8-diarylnaphthalenes

arrangement of all fragments that composes the targeted architectures (ii) the contribution of steric effects and electronic repulsion between *ortho*-substituents and sulphur lone pairs. In addition, our study contributes to a better understanding of key parameters that govern the success or failure to prepare fluorenone or fluorene derivatives starting from common (dihydro)naphthothiophene precursors.

## Results and discussion,

### Synthesis of naphthothiophene platforms

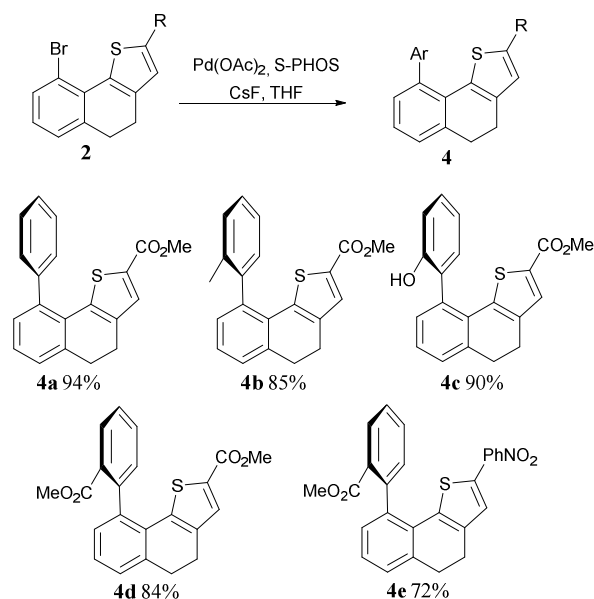
Our first goal was the preparation of aryl naphthothiophene derivatives. We envisioned the preparation of such targets through a three step sequence from 8-bromo tetralone. As recently described,<sup>8</sup> starting chloroacrolein **1** is readily obtained under Vilsmeier-Haack reaction conditions (DMF, POCl<sub>3</sub>, 60°C 3h) in 96% yield.<sup>8,10</sup> The construction of the thiophene ring was realized from **1** through a one-step addition-elimination-cyclization sequence using either methylthioglycolate, pyridine, triethylamine at 50°C or sodium sulfide, *p*-nitrophenyl substituted bromomethylene derivatives and sodium methylate allowing the installation of methoxycarbonyl and *p*-nitrophenyl groups respectively (scheme 1). Various appended dihydronaphthothiophenes **2a** and **2b** were obtained in good to high yield (96%).



**Scheme 1.** Preparation of (dihydro)naphthothiophene platforms.

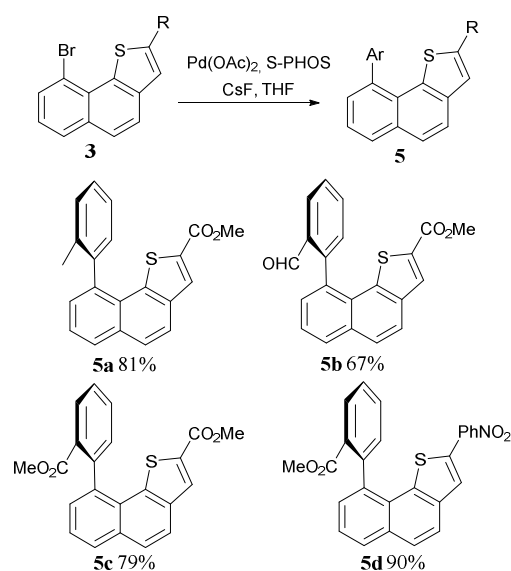
From cornerstone thiophenes **2**, the preparation of aryl naphthothiophenes **3** was achieved using DDQ in refluxing toluene for 2-4h. Having in view the comparison of skeleton topology of the naphthothiophene backbone, we decided to install various aryl groups at the peri position of the naphthalene core in both aromatic (compounds **3**) and partially hydrogenated (compounds **2**) series. Thus starting from dihydronaphthothiophene **2a** as a model compound, several catalytic systems as well as conditions were tested using phenylboronic acid (scheme 2). The use of Pd(OAc)<sub>2</sub>/S-Phos (0.1/0.2 eq.), CsF (4eq.) in refluxing THF was found superior to PdCl<sub>2</sub>, K<sub>2</sub>CO<sub>3</sub> in toluene/water/ethanol, Pd(PPh<sub>3</sub>)<sub>2</sub>Cl<sub>2</sub>, K<sub>2</sub>CO<sub>3</sub> in toluene/water/ethanol or PdppfCl<sub>2</sub>, Cs<sub>2</sub>CO<sub>3</sub> (3eq.) in toluene.

Under such coupling conditions phenylation took place conveniently affording **4a** in 94% yield. Several other boronic acids were coupled in order to install various substituents on the phenyl group such as methyl, hydroxyl, and carbomethoxy group. High yields ranging from 75 to 94% were obtained. The same catalytic system was found to be effective for the introduction of aryl groups on precursors **2b**, leading to **4e** in 72% yield.



**Scheme 2.** Preparation of aryl dihydronaphthothiophenes **4**.

We next moved to the fully aromatic compounds **3** (scheme 3). A similar screening of Pd catalyst was realized in order to set best conditions. Again Pd(OAc)<sub>2</sub>/S-Phos (0.1/0.2 eq.), CsF (4eq.) in refluxing THF represented the best catalytic compromise. We were thus able to install methyl, methoxycarbonyl and carboxaldehyde substituents on the aryl naphthothiophene moiety in high yields (67-90%) starting either from **3a** or **3b**.



**Scheme 3.** Preparation of aryl naphthothiophenes **5**.

We recently showed that methoxycarbonyl derivatives **4d** and **5c** can be readily cyclised into the corresponding fluorenones under Brønsted acid conditions in high yield (figure 2).<sup>8</sup> In this context, we were also interested in preparing the fluorene analogues. A similar sequence involving closely related benzylic alcohols and further electrophilic-type ring closure is expected to afford the fluorene backbone.<sup>11</sup>

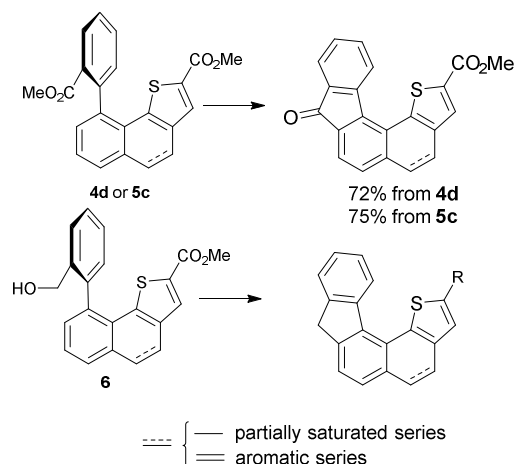
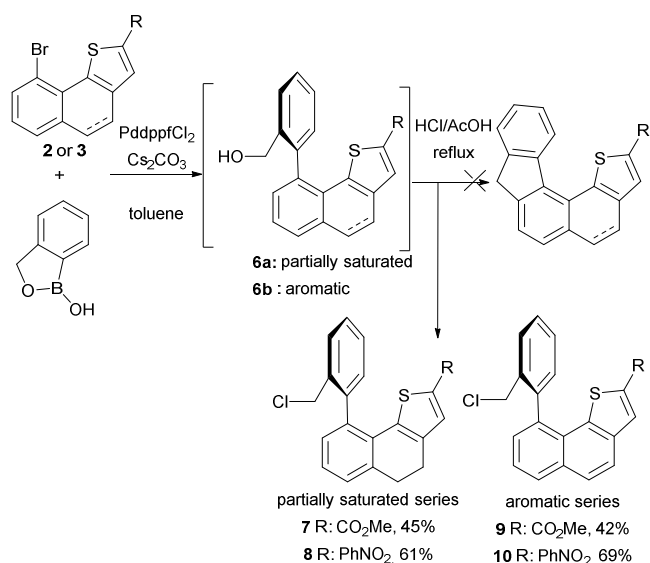


**Figure 2.** Possible pathway towards fluorene backbones.

We next envisioned the preparation of key benzylic alcohols **6**, starting from bromonaphthothiophenes **2** and **3**, (2-hydroxymethyl)phenylboronic acid cyclic monoester under Suzuki-Miyaura coupling conditions. Disappointingly, the use of Pd(OAc)<sub>2</sub>/S-Phos/CsF as the catalytic combination led to poor results mainly affording debrominated side products.



**Scheme 4.** Preparation of chloromethylated naphthothiophenes **7-10**.

In contrast, Pd(dppf)Cl<sub>2</sub>/Cs<sub>2</sub>CO<sub>3</sub> in refluxing toluene led to the expected benzylic alcohols (scheme 4). In almost all cases, the starting bromo derivative was almost entirely converted into alcohols

**6**. The latter intermediates were shortly filtered through a celite pad and directly used in the further cyclization step. Unfortunately, refluxing benzylic alcohols in HCl/AcOH mixture did not afford the expected fluorenes even after prolonged reaction courses. Although <sup>1</sup>H NMR spectra of crude material revealed the presence of characteristic signals that account for two benzylic protons, in all cases only chloromethyl derivatives **7-10** were isolated in yields ranging from 45 to 69%. Attempts to promote the cyclization towards the fluorene scaffold under Lewis acid conditions using AlCl<sub>3</sub> or FeCl<sub>3</sub> failed leading to sluggish residues. It is worth noting that under such conditions, traces of partial hydrolysis of the ester function into their corresponding carboxylic acid may be observed in both aromatic and partially saturated series e.g. compounds **7** and **9**. In addition, chlorides **7-10** exhibit low stability even at low temperature storage. In order to gain information about the overall topology of these series of molecular architectures and shed light on the issues of the ring closure sequence from esters **4d** and **5c** or from benzylic alcohols **6**, we next examined evidences supplied from solid state informations and theoretical calculations.

### Crystal structures

Single crystals suitable for X-ray analysis were obtained by slow evaporation of a DCM solutions of compound **4a**, **4c**, **4d**, **5c**, **8** and **10** (Figure 3 and SI).<sup>12</sup>

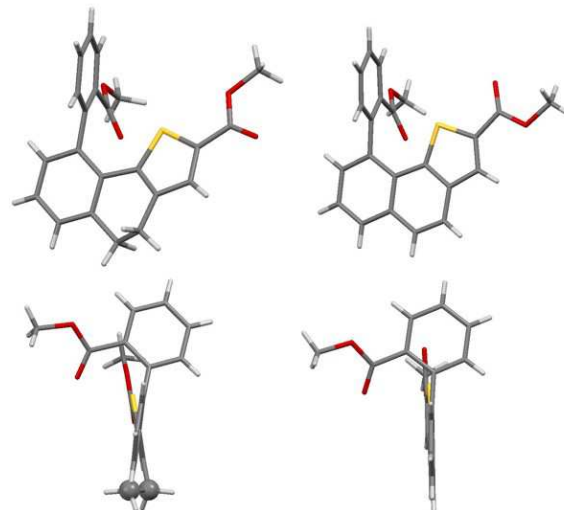


**Figure 3.** X-ray structure of compounds **4d** (left) and **5c** (right).

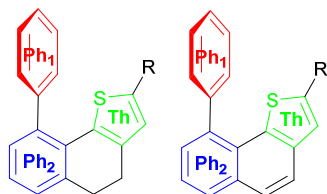
The molecular shape is mainly governed by the saturated bridge for compounds **4a**, **4c**, **4d** and **8** since it induces a non-planar structure (see angle Ph<sub>2</sub>-Th in Table 1). The torsion angle between the mean planes of the phenyl ring and the thiophene one ranges from 15° to 24°. On the other hand when the bridge is unsaturated (compounds **5c** and **10**), the structure is almost planar (5 and 7° deviation).

The second feature of the structures is the relative orientation of the two phenyl rings. It can be analysed by the angle between the mean planes of Ph<sub>1</sub> and Ph<sub>2</sub> in Table 1. In all cases except **4c**, both rings are close to orthogonality and no conjugation can take place. The smaller angle for **4c** (63°) results from the formation of a dimeric structure in the crystal where hydrogen bonds are established

between the OH group and the carbonyl of the ester on the thiophene (see SI figure S3).

It is also noteworthy that the adjacent phenyl ring does not bend away from the sulphur atoms as seen from the short distance between the centroid of Ph<sub>1</sub> and S (3.3 to 3.5 Å). There is no electronic repulsion between the two moieties in these molecules unlike the cofacial case on a naphthalene platform indicated in the introduction.

**Table 1.** Main structural features obtained from X-ray analysis.



Compound	Angle Ph <sub>1</sub> -Ph <sub>2</sub> (°)	Angle Ph <sub>2</sub> -Th (°)	d Ph <sub>1</sub> -S (Å)
<b>4a</b>	90	19	3.36
<b>4c</b>	63	24	3.51
<b>4d</b>	78	17	3.56
<b>5c</b>	81	5	3.34
<b>8</b>	74	15	3.41
<b>10</b>	74	7	3.37

The last topological feature that is interesting in the partially saturated series is the relative orientation of the ethylene bridge. Namely the hydrogen atoms adopt an axial-equatorial arrangement. In **4d** and **8** the CH<sub>2</sub> linked to Ph<sub>2</sub> adopt an arrangement in which the axial hydrogen lies on the opposite side with respect to the substituent on Ph<sub>1</sub>. In contrast, **4d** displays axial hydrogen and the substituent on Ph<sub>1</sub> on the same side. Thus there is no discernible trend at this stage concerning a preferred orientation for the ethylene bridge.

### Theoretical calculations

In order to gain further insight into the preferred geometrical arrangement of these molecules, quantum chemical calculations have been done at the b3lyp/6-31g(d) level of theory to analyse the various conformers and compare them to the structures gained from the solid state analysis. Representation of the minima obtained for all compounds are shown in supporting information together with an overlay with the crystal structure when available. In most cases, a very good agreement was obtained between calculated and experimental structures (Table 2).

The only molecule for which calculated structure differs markedly from the experimental one is **4a**. In the crystal structure, phenyl rings Ph<sub>1</sub> and Ph<sub>2</sub> are orthogonal while in the calculated structure they form an angle of 68°. The feature was ascertained by using the long range corrected functional cam-b3lyp where a Ph<sub>1</sub>-Ph<sub>2</sub> angle of 73° was obtained. The energy of the conformation in the crystal structure was found to be only 3.5 kJ/mol higher than the minimum one. The preferred orientation in the crystal structure could thus come from

intermolecular interactions rather than an intramolecular stabilization.

**Table 2.** Main structural features obtained from geometry optimization (b3lyp/6-31g(d); see table 1 for meaning of Ph<sub>1</sub> Ph<sub>2</sub> and Th).

Compound	Angle Ph <sub>1</sub> -Ph <sub>2</sub> (°)	Angle Ph <sub>2</sub> -Th (°)	d Ph <sub>1</sub> -S (Å)
<b>4a</b>	68	20	3.57
<b>4a<sup>a</sup></b>	73	21	3.52
<b>4b</b>	79	19	3.50
<b>4c</b>	69	20	3.55
<b>4d</b>	81	19	3.59
<b>4e</b>	83	18	3.51
<b>5a</b>	86	2	3.44
<b>5b</b>	86	1	3.46
<b>5c</b>	89	1	3.47
<b>5d</b>	90	1	3.49
<b>6a<sup>b</sup></b>	87	17	3.49
<b>6b<sup>b</sup></b>	86	2	3.47
<b>7</b>	83	18	3.50
<b>8</b>	84	17	3.48
<b>9</b>	87	1	3.44
<b>10</b>	87	1	3.43

<sup>b</sup> cam-b3lyp/6-31g(d);

It appears that in most cases, the overall minimum in the gas phase is closely related to the crystal structure. It was thus interesting to study the effect of changing the relative orientation of the CH<sub>2</sub>-CH<sub>2</sub> bridge in the aliphatic series. Three compounds were studied (**4a**, **4c** and **8**) where the size of the substituent on Ph<sub>1</sub> increases (see SI). In all cases, the inversion gave final structures whose energy was close to the initial one (maximum difference observed is 2.3 kJ/mol and 2.6 kJ/mol with b3lyp and cam-b3lyp functionals respectively). Furthermore, the energy barrier was found to be *ca.* 20kJ/mol in all three cases whatever the functional used. The preference for one orientation in the crystal structure comes from small energy differences and it is likely that in solution both conformations exist and exchange. This is substantiated by the NMR data where a single signal is found for each CH<sub>2</sub> group indicating that on the NMR timescale both protons occupies both axial and equatorial positions.

Another interesting feature to study in this series was the rotation around the C-C bond linking the two phenyl rings since blocking it, could open the way to the preparation of optically active compounds. It was studied in four representative cases: **4b**, **4c**, **5a** and **8**. The rotation barrier was found to be high in all cases (96, 116, 103 and 105 kJ/mol respectively).<sup>13</sup> It is noteworthy that the nature of the bridge (saturated or not) has no influence (**4b** vs **5a**) and that a methyl or hydroxyl substituent are already large enough to block this rotation at room temperature.

Finally, we also had a look at the electronic factors governing the stability of the structure. It was noted that in the crystal structures of the compounds, the Ph<sub>1</sub>-S distance is short and the phenyl ring does not bend away. This feature was reproduced by the geometry optimization (Table 2). The electrostatic

potential surfaces were plotted (figure 4) and it was found that an electron dense region exists in between the face of the phenyl and the sulphur atom.

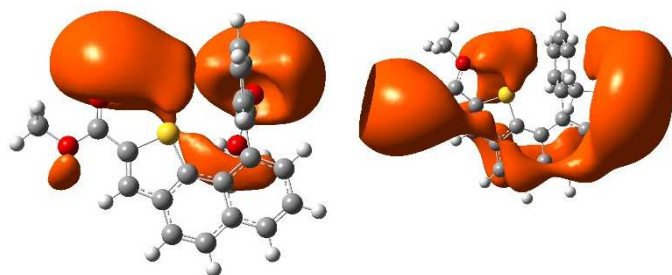


**Figure 4.** Electrostatic potential surfaces for compounds **5c** and **9** (orange = negative regions, positive regions have been omitted for clarity). Sulfur atom is in yellow.

Natural Bond Orbital (NBO) calculation<sup>14</sup> was also performed since it was proven to be a very useful tool to study the electronic properties of organic molecules. We focused on the delocalization energies between the two moieties (Second Order Perturbation Theory Analysis). It was found that the  $\pi$  electrons of the phenyl ring interact with the vacant d orbitals of the sulphur atom explaining the short distance observed and the apparent lack of electronic repulsion which was observed in the bisaryl naphthalene case.

#### Determination of key factors in the ring closure sequence

In order to understand the difference of reactivity between compounds **4d** and **5c** on one hand which allow obtaining the corresponding fluorenones and compounds **6a-b** on the other hand that failed to give the fluorene analogues, geometry optimizations have been realized. Comparison of key data showed no major geometrical differences between **4d** or **5c** and **6a-b** that could explain the lesser reactivity of the latter (Table 2 and SI). However, further insight could be gained by studying the carbocations which are believed to be the reactive intermediates. Inspection of the lowest unoccupied molecular orbitals (LUMO) did not deliver useful information since both show that the electron density is localized on the reactive carbon with a delocalization into the adjacent phenyl ring (see SI). On the other hand, the highest occupied molecular orbitals (HOMO) show significant differences (Figure 5). In the case of **5c**, the HOMO has an electron density on the carbon in *ortho* position which is the electrophilic aromatic substitution site but in the case of **9**, the electron density on the same carbon site is much weaker.

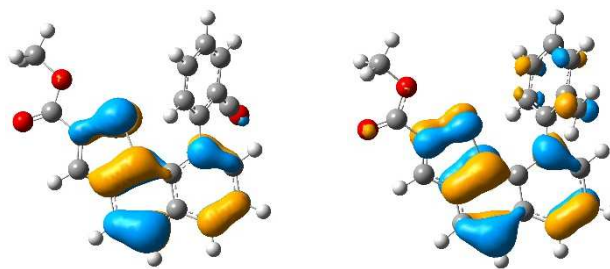


**Figure 5.** Highest occupied molecular orbitals of the cation of compounds **5c** (left) and **9** (right).

This difference in electron density could explain the difference of reactivity when attempting to form the fluorenone or the fluorene. In the latter case alternative synthetic approaches are needed.<sup>15</sup>

Further insight into the reactivity of both series was obtained by studying the reaction path leading to cyclisation or formation of the benzylchloride. The SEAr reaction from the carbocation of **4d** or **5c** was found to be easily achieved with activation energies of 5.6 and 6.5 kcal/mol respectively.

The cyclisation of carbocations of **6a-b** in saturated and unsaturated series were found to be rather easy to perform as well since the activation energies for the electrophilic reaction are 11.0 and 9.2 kcal/mol respectively. The  $S_N1$  reaction was found to require slightly more energy ( $E_a = 15.1$  and 15.2 kcal/mol). However the  $S_N1$  product is much more stable than the SEAr one by 83 and 95 kcal/mol respectively (figure 6 for **7** and SI for **9**)

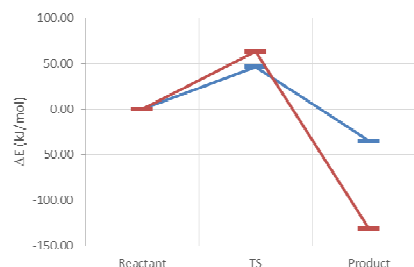


**Figure 6.** Reaction pathways from the carbocation of **6a** leading to potential cyclisation (SEAr in blue) or formation of **7** ( $S_N1$  in red).

DFT calculations thus indicate that in the case of compound **6** the formation of the fluorene is an equilibrated reaction and that at high temperature the thermodynamically favourable product arising from  $S_N1$  reaction is obtained predominantly.

#### Conclusions

In summary, we succeeded in the preparation of several naphtho- and dihydronaphthothiophene derivatives in two key steps. The first step allowed building up the condensed thiophene ring starting from a common  $\beta$ -chloro acrolein derivative. The second step aimed at the installation of various aryl groups using a Suzuki-Miyaura coupling reaction. The overall topology of these architectures has been confirmed by X-ray analyses. Key parameters that impact the preferred

geometrical shape of such molecular platforms have been determined through quantum chemical calculations. Furthermore, ring closure sequences in order to prepare thienyl-fused fluorenes have been examined. In deep contrast to the fluorenones series, fluorenes could not be obtained using similar intramolecular electrophilic aromatic processes. The lack of reactivity of benzylic alcohols precursors, by comparison with their methoxycarbonyl analogues, originates from a marked difference of electronic densities at the cyclisation sites which could be determined through geometry optimization calculations. Reactions pathways and issues selectively leading to the corresponding fluorenones on one hand and to benzylchlorides on the other hand have been characterized.

### Acknowledgements

The authors are grateful to the University of Versailles Saint Quentin-en-Yvelines, ENS Cachan, CEA-Saclay, the Tunisian Ministry of Higher Education, Scientific Research and Technology, ANR (ANR-11-BS07-030-01) and IDEX Paris-Saclay for the financial support and grant (HB).

### Experimental

#### Materials and methods

Unless otherwise noted, all starting materials were obtained from commercial suppliers and used without purification. Petroleum ether was distilled under Argon. NMR spectra were recorded on a 300 MHz and 200 MHz Bruker spectrometers. Chemical shifts were reported in ppm relative to the residual solvent peak (7.27 ppm for CHCl<sub>3</sub>) for <sup>1</sup>H spectra and (77.00 ppm for CDCl<sub>3</sub>) for <sup>13</sup>C spectra. High Resolution Mass spectroscopy data were recorded on an Autospec Ultima (Waters/Micromass) device with a resolution of 5000 RP at 5%. Compounds **1**, **2a**, **3a**, **4d**, **5c** were prepared according to reference 8. Thin-layer chromatography (TLC) was carried out on aluminium sheets precoated with silica gel 60 F254. Column chromatography separations were performed using silica gel (0.040-0.060 mm).

Calculations were performed using Gaussian 09 software.<sup>16</sup> Molecules structures were drawn with Gaussview software using included templates and their geometry optimized at the b3lyp/6-31g(d) level of theory and additionally at the cam-b3lyp/6-31g(d) level for **4a**. A frequency job was done on the final geometry to ascertain that a minimum was obtained (no negative frequencies). Scan (opt=modredundant) were done at the b3lyp/6-31g(d) and cam-b3lyp/6-31g(d) level of calculations. NBO analysis were performed after an energy calculation at the B3LYP/6-311+g(d,p) level of theory.

#### Synthetic procedures

##### Procedure for synthesis of compound **2b**.

Compound **1** (0.18 mmol) in 1 mL DMF was added to a suspension of sodium sulfide (0.2 mmol) in 1 mL DMF at room temperature. After 15 min, paranitrobenzylbromide (0.18 mmol) was added. After further 15 min, sodium methoxide (0.18 mmol) was added and after 10 min of stirring at rt, the mixture was extracted with methylene chloride. The resulting methylene chloride solution was dried over anhydrous

magnesium sulfate and the solvent was removed under reduced pressure. The crude product was purified by flash chromatography on silica gel eluting with petroleum ether/ethyl acetate (95:5) to yield compound **2b** and **2c** in 69 and 77% respectively.

##### Compound **2b** (69%)

<sup>1</sup>H NMR (300 MHz, CDCl<sub>3</sub>): δ = 2.83-2.90 (m, 2H), 2.96-3.05 (m, 2H), 7.03 (t, *J* = 7.7 Hz, 1H), 7.24 (d, *J* = 10.2 Hz, 1H), 7.36 (s, 1H), 7.55 (d, *J* = 7.7 Hz, 1H), 7.81 (d, *J* = 8.9 Hz, 2H), 8.25 (d, *J* = 9 Hz, 2H).

<sup>13</sup>C NMR (75 MHz, CDCl<sub>3</sub>): δ = 24.3, 30.8, 119.6, 124.4, 125.1, 125.7, 127.4, 127.8, 131.1, 132.8, 135.6, 138.7, 140.2, 140.6, 142.1, 146.5.

HRMS-ESI: *m/z* [M + H]<sup>+</sup> calcd for C<sub>18</sub>H<sub>12</sub>NO<sub>2</sub>SBr: 384.9772; found: 384.9771.

##### Preparation of compound **3b**.

Compound **2b** (26 mg, 0.06 mmol) and DDQ (22 mg, 0.096 mmol) were dissolved in toluene (2 mL) and heated at reflux for 2 h. After cooling to room temperature, the resulting solution was concentrated under reduced pressure and purified by flash chromatography on silica gel eluting with petroleum ether/ethyl acetate (90:10) to yield to **3b** as a yellow solid in 90% yield.

<sup>1</sup>H NMR (300 MHz, CDCl<sub>3</sub>): δ = 7.37 (t, *J* = 7.7 Hz, 1H), 7.79 (m, 3H), 7.91 (m, 4H), 8.26 (d, *J* = 9 Hz, 2H).

<sup>13</sup>C NMR (75 MHz, CDCl<sub>3</sub>): δ = 120.4, 123.1, 124.0, 125.1 (2), 126.7, 127.5 (2), 127.7, 129.3, 129.7, 130.3, 133.1, 134.5, 137.1, 137.4, 141.1, 142.5.

HRMS-ESI: *m/z* [M + H]<sup>+</sup> calcd for C<sub>18</sub>H<sub>10</sub>NO<sub>2</sub>SBr: 382.9616; found: 382.9609.

##### General procedure for S-Phos catalyzed Suzuki-Miyaura coupling

To a stirred suspension of 9-bromonaphtho[1,2-b]thiophene derivative (0.40 mmol), boronic acid (0.81 mmol, 2 eq.), and cesium fluoride (247 mg, 1.6 mmol, 4eq.) in degassed THF (4 mL), were added palladium acetate (9.1 mg, 0.04 mmol) and 2-dicyclohexylphosphino-2',6'-dimethoxybiphenyl (33.3 mg, 0.08 mmol). The mixture was heated at reflux in THF for 2h. Water (20 mL) was then added, and the aqueous phase was extracted with methylene chloride (3 x 20 mL). The combined organic layers were dried over anhydrous magnesium sulfate, filtered, and concentrated under vacuum. The crude product was purified by flash chromatography on silica gel eluting with petroleum ether/ethyl acetate (9:1) or petroleum ether/methylene chloride (6:4) to give the coupling product.

##### Compound **4a** (94%)

<sup>1</sup>H NMR (300 MHz, CDCl<sub>3</sub>): δ = 2.81-2.86 (m, 2H), 2.96-3.01 (m, 2H), 3.76 (s, 3H), 7.11 (dd, *J* = 2, 7 Hz, 1H), 7.20-7.32 (m, 3H), 7.44-7.46 (m, 2H), 7.49 (s, 1H).

<sup>13</sup>C NMR (75 MHz, CDCl<sub>3</sub>): δ = 24.7, 30.8, 52.5, 128.0, 128.2, 129.1, 129.5, 130.0, 130.1, 130.7, 132.0, 132.95, 137.8, 139.8, 140.1, 141.5, 142.4, 163.8.

HRMS-ESI: *m/z* [M + H]<sup>+</sup> calcd for C<sub>20</sub>H<sub>17</sub>O<sub>2</sub>S : 321.0949; found: 321.0945.

**Compound 4b** (85%)

<sup>1</sup>H NMR (300 MHz, CDCl<sub>3</sub>): δ = 2.00 (2s, 3H), 2.82-2.86 (m, 2H), 2.98-3.03 (m, 2H), 3.76 (2s, 3H), 7.04-7.07 (m, 1H), 7.19 (d, *J* = 7.7 Hz, 1H), 7.22-7.28 (m, 4H), 7.38-7.42 (m, 1H), 7.54 (s, 1H).

<sup>13</sup>C NMR (75 MHz, CDCl<sub>3</sub>): δ = 19.8, 23.9, 30.1, 51.8, 126.4, 127.3, 127.4, 128.7, 128.8, 129.2, 130.0, 130.4, 131.1, 132.2, 136.7, 136.8, 138.0, 139.0, 139.9, 141.6, 163.1.

**HRMS-ESI:** *m/z* [M + H]<sup>+</sup>calcd for C<sub>21</sub>H<sub>19</sub>O<sub>2</sub>S: 335.1106; found: 335.1109.

**Compound 4c** (90%)

<sup>1</sup>H NMR (200 MHz, CDCl<sub>3</sub>): δ = 2.82-2.89 (m, 2H), 2.98-3.05 (m, 2H), 3.76 (s, 3H), 4.72 (s, 1H), 7.00 (dd, *J* = 0.7, 8.0 Hz, 2H), 7.15-7.18 (m, 2H), 7.29-7.33 (m, 2H), 7.41 (td, 1.9, 8 Hz, 1H), 7.50 (s, 1H).

<sup>13</sup>C NMR (75 MHz, CDCl<sub>3</sub>): δ = 24.7, 30.9, 52.7, 116.9, 122.2, 127.3, 128.9, 129.5, 130.9, 131.4, 131.5, 131.8, 132.7, 132.9, 133.1, 138.4, 140.33, 141.3, 154.1, 163.7.

**HRMS-ESI:** *m/z* [M + H]<sup>+</sup>calcd for C<sub>20</sub>H<sub>17</sub>O<sub>3</sub>S: 337.0898; found: 337.0901.

**Compound 4e** (72%)

<sup>1</sup>H NMR (300 MHz, CDCl<sub>3</sub>): δ = 2.80-2.88 (m, 2H), 2.96-3.09 (m, 2H), 3.51 (s, 3H), 7.02 (d, *J* = 7.5 Hz, 1H), 7.11-7.18 (m, 3H), 7.25-7.28 (m, 1H), 7.35 (d, *J* = 9 Hz, 2H), 7.50-7.53 (m, 2H), 8.09-8.14 (m, 3H).

<sup>13</sup>C NMR (75 MHz, CDCl<sub>3</sub>): δ = 24.3, 30.2, 51.9, 124.2, 125.1, 125.2, 126.4, 127.3, 128.1, 128.5, 129.1, 130.7, 131.1, 132.1, 132.2, 135.8, 137.6, 139.7, 140.4, 140.7, 142.0, 146.1, 167.0.

**HRMS-ESI:** *m/z* [M]<sup>+</sup>calcd for C<sub>26</sub>H<sub>19</sub>NO<sub>4</sub>S: 441.1035; found: 441.1026.

**Compound 5a** (81%)

<sup>1</sup>H NMR (300 MHz, CDCl<sub>3</sub>): δ = 1.85-1.89 (2s, 3H), 3.66-3.74 (2s, 3H), 7.14-7.16 (m, 1H), 7.26-7.34 (m, 3H), 7.39 (t, *J* = 1.3, 7.6 Hz, 1H), 7.53 (t, *J* = 7.9, 15.2 Hz, 1H), 7.73 (s, 2H), 7.86 (d, *J* = 7.9 Hz, 1H), 7.95 (s, 1H).

<sup>13</sup>C NMR (75 MHz, CDCl<sub>3</sub>): δ = 19.8, 52.2, 123.0, 126.2, 126.7, 126.8, 127.4, 128.2, 128.5, 129.2, 130.2, 130.3, 130.8, 132.8, 133.4, 137.5, 137.7, 138.4, 139.9, 140.0, 163.3.

**HRMS-ESI:** *m/z* [M + H]<sup>+</sup>calcd for C<sub>21</sub>H<sub>17</sub>O<sub>2</sub>S: 333.0949; found: 333.0937.

**Compound 5b** (67%)

<sup>1</sup>H NMR (300 MHz, CDCl<sub>3</sub>): δ = 3.84 (s, 3H), 7.45-7.52 (m, 2H), 7.60-7.69 (m, 1H), 7.74-7.81 (m, 2H), 7.88 (s, 2H), 8.05 (d, *J* = 1.2 Hz, 1H), 8.07 (s, 1H), 8.1 (dd, *J* = 2.0, 7.1 Hz, 1H), 9.63 (s, 1H).

<sup>13</sup>C NMR (75 MHz, CDCl<sub>3</sub>): δ = 52.3, 123.5, 125.7, 126.8, 127.6, 128.1, 129.4, 129.5, 129.7, 130.3, 131.8, 132.6, 133.6, 134.3, 134.5, 135.1, 138.1, 139.6, 143.7, 162.9, 191.3.

**HRMS-ESI:** *m/z* [M]<sup>+</sup>calcd for C<sub>21</sub>H<sub>14</sub>O<sub>3</sub>S: 346.0664; found: 346.0664.

**Compound 5d** (90%)

<sup>1</sup>H NMR (300 MHz, CDCl<sub>3</sub>): δ = 3.47(s, 3H), 7.37 (d, *J* = 7.1 Hz, 1H), 7.42-7.45 (m, 1H), 7.53-7.66 (m, 3H), 7.70-7.73 (m, 3H), 7.85 (s, 2H), 7.99 (d, *J* = 8.1 Hz, 1H), 8.19 (d, *J* = 8.8 Hz, 2H), 8.23-7.26 (m, 1H).

<sup>13</sup>C NMR (75 MHz, CDCl<sub>3</sub>): δ = 51.8, 122.2, 122.4, 124.2 (2), 125.1, 126.3 (2), 126.9, 127.1, 127.2, 128.5, 128.9, 131.0, 131.2, 131.8, 132.5 (2), 137.2, 138.1, 139.3, 140.6, 141.1, 141.9, 146.7, 166.7.

**HRMS-ESI:** *m/z* [M]<sup>+</sup>calcd for C<sub>26</sub>H<sub>17</sub>NO<sub>4</sub>S: 439.0878; found: 439.0880.

General procedure for dppf catalyzed Suzuki-Miyaura coupling – chlorination sequence affording compounds **7-10**.

To a stirred suspension of methyl 9-bromo-4,5-naphtho[1,2-*b*]thiophene derivative (0.31 mmol), (2-hydroxymethyl)phenylboronic acid cyclic monoester (1.22 mmol, 4 eq.), and Cs<sub>2</sub>CO<sub>3</sub> (300 mg, 0.92 mmol,) in degassed mixture of toluene (3 mL), was added 1,1'-bis(diphenylphosphino)ferrocene[dichloropalladium (35 mg, 0.047 mmol). The mixture was stirred at reflux for 1h. Water (20 mL) was then added, and the aqueous phase was extracted with methylene chloride (3 x 20 mL). The combined organic layers were dried over anhydrous magnesium sulfate, filtered, and concentrated under vacuum. The crude product was filtered through a pad of silica gel. The resulting mixture was checked by <sup>1</sup>H NMR and further reacted with a mixture of HCl/Acetic acid (2/1 mL) and stirred at room temperature for 2 h. The resulting mixture was then poured into ice (20 g) and basified with sodium bicarbonate. This aqueous layer was extracted with ethyl acetate (3 x 20 mL). The combined organic layers were dried over anhydrous magnesium sulfate, filtered and concentrated under vacuum. The crude product was purified by flash chromatography on silica gel eluting with methylene chloride then ethyl acetate/ methanol (90:10).

**Compound 7** (45%)

<sup>1</sup>H NMR (300 MHz, CDCl<sub>3</sub>): δ = 2.73-2.78 (m, 2H), 2.90-2.95 (m, 2H), 3.67 (s, 3H), 4.21-4.32 (m, 2H), 6.98-7.01 (m, 1H), 7.12-7.19 (m, 3H), 7.30-7.35 (m, 1H), 7.40-7.47 (m, 2H), 7.52 (d, *J* = 7.9 Hz, 1H).

<sup>13</sup>C NMR (75 MHz, CDCl<sub>3</sub>): δ = 24.0, 30.2, 51.9, 63.1, 127.5, 127.7, 127.8, 128.1, 128.2, 129.1, 129.4, 130.4, 131.5, 132.4, 136.5, 137.0, 138.8, 139.4, 141.2, 162.9.

**HRMS-ESI:** *m/z* [M + H]<sup>+</sup>calcd for C<sub>21</sub>H<sub>18</sub>O<sub>2</sub>SCl: 369.0716; found: 369.0722.

**Compound 8** (61%)

<sup>1</sup>H NMR (300 MHz, CDCl<sub>3</sub>): δ = 2.89-2.95 (m, 2H), 3.02-3.08 (m, 2H), 4.32-4.42 (m, 2H), 7.14-7.31 (m, 5H), 7.44 (d, *J* = 8.8 Hz, 2H), 7.56-7.63 (m, 3H), 8.14 (d, *J* = 8.9 Hz, 2H).

<sup>13</sup>C NMR (75 MHz, CDCl<sub>3</sub>): δ = 24.2, 30.1, 44.1, 124.2 (2), 125.1, 125.2 (2), 126.7, 127.9, 128.9, 129.2, 129.3, 129.6, 130.2, 131.0, 135.1, 136.2, 136.3, 136.7, 140.0, 140.1, 140.5, 140.7, 146.1.

**HRMS-ESI:** *m/z* [M]<sup>+</sup>calcd for C<sub>25</sub>H<sub>18</sub>NO<sub>2</sub>SCl: 431.0747; found: 431.0741.

**Compound 9** (42%)

<sup>1</sup>H NMR (300 MHz, CDCl<sub>3</sub>): δ = 3.85 (s, 3H), 3.963 (d, *J* = 11.6 Hz, 1H), 4.32 (d, *J* = 11.6 Hz, 1H), 7.29 (d, *J* = 7.2 Hz, 1H), 7.51-7.72 (m, 5H), 7.87 (s, 2H), 8.05 (d, *J* = 8.1 Hz, 1H), 8.07 (s, 1H).

<sup>13</sup>C NMR (75 MHz, CDCl<sub>3</sub>): δ = 44.0, 52.3, 123.2, 126.0, 129.9, 127.4, 129.3, 129.4, 129.9, 130.3, 130.6, 131.1, 132.8, 133.5, 135.9, 136.7, 138.0, 139.7, 139.8, 163.2.

HRMS-ESI: *m/z* [M]<sup>+</sup> calcd for C<sub>21</sub>H<sub>15</sub>O<sub>2</sub>SCl: 366.0481; found: 366.0487.

**Compound 10** (69%)

<sup>1</sup>H NMR (300 MHz, CDCl<sub>3</sub>): δ = 4.18 (d, *J* = 11 Hz, 1H), 4.38 (d, *J* = 11 Hz, 1H), 7.38 (d, *J* = 7.4 Hz, 1H), 7.53-7.74 (m, 8H), 7.88 (s, 2H), 8.05 (d, *J* = 8.1 Hz, 1H), 8.22 (d, *J* = 8.2 Hz, 1H).

<sup>13</sup>C NMR (75 MHz, CDCl<sub>3</sub>): δ = 44.3, 122.5, 122.6, 122.8 (2), 124.5, 125.6 (2), 126.6, 128.9, 129.3, 129.5, 129.9, 130.6, 131.3, 131.6, 132.4, 134.7, 135.6, 137.2, 139.7, 140.2, 140.7, 141.8, 147.1.

HRMS-ESI: *m/z* [M]<sup>+</sup> calcd for C<sub>25</sub>H<sub>16</sub>NO<sub>2</sub>SCl: 429.0597; found: 429.0594.

**Notes and references**

<sup>a</sup> Université de Versailles Saint Quentin-en-Yvelines, Institut Lavoisier de Versailles - UMR CNRS 8180, 45, avenue des Etats-Unis, 78035 Versailles Cedex, France.

<sup>b</sup> CEA Saclay, SCBM, iBiTec-S, Building 547, PC # 108, 91191 Gif sur Yvette, France.

<sup>c</sup> Faculté des Sciences de Monastir, Laboratoire de Synthèse Organique, Asymétrique et Catalyse Homogène (URES56), Avenue de l'Environnement, 5019 Monastir, Tunisia.

<sup>d</sup> ENS-Cachan, PPSM-UMR CNRS 853, Bâtiment d'Alembert, 61, avenue du Président Wilson 94235 CACHAN Cedex, France.

† Footnotes should appear here. These might include comments relevant to but not central to the matter under discussion, limited experimental and spectral data, and crystallographic data.

Electronic Supplementary Information (ESI) available: [details of any supplementary information available should be included here]. See DOI: 10.1039/b000000x/

- For review and recent papers see: D. Xiao, Z. Zhang and X. Zhang, *Org. Lett.*, 1999, **1**, 1679-1681. L. Pu, *Chem. Rev.*, 1998, **98**, 2405-2494. S. Ge, R. A. Green and J. F. Hartwig, *J. Am. Chem. Soc.*, 2014, **136**, 1617-1627. R. Horikoshi, *J. Chem. Educ.*, 2015, **92**, 332-335. Y. Sakaguchi, N. Kurono, K. Yamauchi and T. Ohkuma, *Org. Lett.*, 2014, **16**, 808-811.
- K. Takaishi and M. Kawamoto, *Molecules*, 2011, **16**, 1603-1624.
- Z.-J. Wang, G.-J. Deng, Y. Li, Y.-M. He, W.-J. Tang and Q.-H. Fan, *Org. Lett.*, 2007, **9**, 1243-1246.
- H. Ghosh, R. Vavilala and A. M. Szpilman, *Tetrahedron: Asymmetry*, 2015, **26**, 79-84.
- D. K. Judge, P. Haycock, R. D. Richardson and M. J. Fuchter, *Synlett*, 2013, **24**, 2365-2369.
- G. Pieters, A. Gaucher, J. Marrot, F. Maurel, J.-V. Naubron, M. Jean, N. Vanthuynne, J. Crassous and D. Prim, *Org. Lett.*, 2011, **13**, 4450-4453. G. Pieters, V. Terrasson, A. Gaucher, D. Prim and J. Marrot, *Eur. J. Org. Chem.*, 2010, 5800-5806. G. Pieters, A. Gaucher, D. Prim and J. Marrot, *Chem. Commun.* 2009, 4827-4828.

- G. Pieters, A. Gaucher, D. Prim, T. Besson, J. Giner Planas, F. Teixidor, C. Vinas, M. E. Light and M. B. Hursthouse, *Chem. Commun.*, 2011, **47**, 7725-7727. E. Celia, S. Amigoni, E. Taffin de Givenchy, G. Pieters, A. Gaucher, D. Prim, J.-F. Audibert R. Méallet-Renault and F. Guittard, *Chem. Commun.*, 2014, **50**, 12034-12036.
- A. Souibgui, A. Gaucher, J. Marrot, F. Aloui, F. Mahuteau-Betzer, B. Ben Hassine and D. Prim, *Eur. J. Org. Chem.*, 2013, 4515-4522.
- S. K. Pal, T. Sahu, T. Misra, T. Ganguly, T. K. Pradhan and A. De, *J. Photochem. Photobiol., A*, 2005, **174**, 138-148. S. K. Pal, S. Bhattacharaya, S. K. Batayal, T. K. Pradhan and T. Ganguly, *J. Photochem. Photobiol., A*, 2007, **189**, 86-93. T. Dutta, Y. Li, A. L. Thornton, D.-M. Zhu and Z. Peng, *J. Polym. Sci., Part A: Polym. Chem.*, 2013, **51**, 3818-3828.
- D. Prim, A. Fuss, G. Kirsch and A. M. S. Silva, *J. Chem. Soc., Perkin Trans 2*, 1999, 1175-1180. G. Kirsch, D. Prim, F. Leising and G. Mignani, *J. Heterocyclic Chem.*, 1994, **31**, 1005-1009.
- For recent example of electrophilic-type cyclisation using HCl see L. Hai, X. Hou, Y. Hua, Y. Huang, B. Zhao, F. Liu, B. Peng, W. Weil and W. Huang, *Org. Lett.*, 2007, **9**, 1619-1622.
- Cambridge Crystallographic Data Center deposition numbers: **4a** (CCDC 1414605); **4c** (CCDC 1414606); **4d** (CCDC 1414607); **5c** (CCDC 919294); **8** (CCDC 1414608); **10** (CCDC 1414609).
- The rotation barrier were also calculated at the cam-b3lyp/6-31g(d) level and were found to be 4 to 7 kJ/mol higher: 100, 123, 108 and 111 kJ/mol for **4b**, **4c**, **5a** and **8** respectively.
- E. D. Glendening, C. R. Landis and F. Weinhold, *WIREs Comput. Mol. Sci.*, 2012, **2**, 1.
- S. J. Hwang, H. J. Kim and S. Chang, *Org. Lett.*, 2009, **11**, 4588-4591.
- Gaussian 09, Revision D.01, M. J. Frisch, G. W. Trucks, H. B. Schlegel, G. E. Scuseria, M. A. Robb, J. R. Cheeseman, G. Scalmani, V. Barone, B. Mennucci, G. A. Petersson, H. Nakatsuji, M. Caricato, X. Li, H. P. Hratchian, A. F. Izmaylov, J. Bloino, G. Zheng, J. L. Sonnenberg, M. Hada, M. Ehara, K. Toyota, R. Fukuda, J. Hasegawa, M. Ishida, T. Nakajima, Y. Honda, O. Kitao, H. Nakai, T. Vreven, J. A. Montgomery, Jr., J. E. Peralta, F. Ogliaro, M. Bearpark, J. J. Heyd, E. Brothers, K. N. Kudin, V. N. Staroverov, T. Keith, R. Kobayashi, J. Normand, K. Raghavachari, A. Rendell, J. C. Burant, S. S. Iyengar, J. Tomasi, M. Cossi, N. Rega, J. M. Millam, M. Klene, J. E. Knox, J. B. Cross, V. Bakken, C. Adamo, J. Jaramillo, R. Gomperts, R. E. Stratmann, O. Yazyev, A. J. Austin, R. Cammi, C. Pomelli, J. W. Ochterski, R. L. Martin, K. Morokuma, V. G. Zakrzewski, G. A. Voth, P. Salvador, J. J. Dannenberg, S. Dapprich, A. D. Daniels, O. Farkas, J. B. Foresman, J. V. Ortiz, J. Cioslowski, and D. J. Fox, Gaussian, Inc., Wallingford CT, 2013.